Kinetics of concurrent desorption and diffusion into the solid: D/Zr(0001)

M. Kovar, K. Griffiths, R. V. Kasza, J. G. Shapter, P. R. Norton, and V. P. Zhdanov

Citation: The Journal of Chemical Physics **106**, 4797 (1997); doi: 10.1063/1.473478
View online: https://doi.org/10.1063/1.473478
View Table of Contents: http://aip.scitation.org/toc/jcp/106/11
Published by the American Institute of Physics

Kinetics of concurrent desorption and diffusion into the solid: D/Zr(0001)

M. Kovar, K. Griffiths, R. V. Kasza, J. G. Shapter, and P. R. Norton
Interface Science Western, Department of Chemistry, University of Western Ontario, London, Ontario N6A 5B7, Canada

V. P. Zhdanov
Department of Applied Physics, Chalmers University of Technology, S-412 96 Göteborg, Sweden, and Boreskov Institute of Catalysis, Russian Academy of Sciences, Novosibirsk 630090, Russia

(Received 20 May 1996; accepted 13 December 1996)

Rapid adsorbate diffusion into the solid is known to suppress the desorption yield measured in a thermal desorption experiment. We show that this suppression can be controlled (at least partly) by pulsed-laser heating at rates in excess of 10^{10} K/s. As an example, we analyze the D/Zr system. In this case, deuterium adsorbed on a surface rapidly diffuses into the bulk of Zr with increasing temperature, and the deuterium desorption probability measured with conventional heating rates ($\beta \leqslant 100$ K/s) is as low as $\approx 10^{-4}$ for polycrystalline Zr foils (deuterium desorption is not observed at all from single-crystal Zr from which dissolved H/D has been removed). Heating the Zr(0001) surface by pulsed-laser thermal excitation with $\beta \simeq 10^{11}$ K/s is demonstrated to result in the increase of the deuterium desorption probability up to approximately 0.01. To interpret this observation, general equations for describing associative desorption accompanied by adsorbate diffusion into the solid are simplified by employing the specifics of the temperature-programmed kinetic regimes with a linear increase of temperature. The desorption yield calculated without any adjustable parameters is in good agreement with the experimental results. © *1997 American Institute of Physics.* [S0021-9606(97)51211-6]

I. INTRODUCTION

Dissociative adsorption of such molecules as H_2, O_2 and N_2 is often accompanied by adsorbate diffusion into the solid and then by formation of subsurface or bulk compounds.[1,2] These processes play an important role in industrial applications and are also of interest from the point of view of different branches of chemical physics including materials science and surface science. For these reasons, it is of particular interest to understand the interplay between diffusion into the bulk and thermal desorption. Obviously, the former process will suppress the latter one. If at conventional heating rates (1–100 K/s) the desorption yield is low, it can be increased if the surface is heated by pulsed-laser excitation at rates in excess of 10^{10} K/s (in analogy with desorption of highly reactive species[3,4]). Experiments of this type have not so far been reported. A theoretical analysis of the laser-induced regime of thermal desorption (LITD) accompanied by adsorbate diffusion into the bulk is also lacking. In the present paper, we report the results of LITD measurements of the concurrent kinetics of desorption and diffusion of deuterium from Zr(0001). This is the *first* application of LITD for this type of study. The data obtained are *quantitative* because we use a novel method of calibration of the LITD signal (the lack of calibration is a weak point in many LITD measurements). In addition, we present general equations for describing the phenomenon under consideration and employ them to interpret *quantitatively* the results of measurements.

The system chosen for our investigation, D/Zr, has attracted considerable attention during the past decade because (i) Zr is widely used as a material for the construction of nuclear reactors and (ii) its bulk properties change dramatically with increasing hydrogen uptake. Experimentally, diffusion of hydrogen/deuterium into the Zr subsurface region and/or into the bulk was observed and studied in Refs. 5–14 (dissociation of O_2,[5,15] N_2,[5] NO,[5] and CO[5] on Zr is also accompanied by absorption of the adsorbates). The rate of hydrogen/deuterium diffusion into the bulk was shown to be high even at room temperature because the activation barrier for this step is fairly low.[10]

Desorption of hydrogen/deuterium has only been reported for experiments on polycrystalline Zr foils.[5,14,16] In particular, Foord *et al.*[5] have registered a D_2 desorption peak maximum at $\simeq 1480$ K for exposures $\leqslant 1$ Langmuir (L). With increasing exposure (up to 1200 L), the peak was broadened and its position shifted to lower temperatures (the origin of this peak was not discussed in detail). The desorption yield (measured in arbitrary units) has been shown to increase linearly with increasing exposure. Lin and Gilbert[16] have registered hydrogen desorption at 1000–1400 K for exposures from 6 to 50 L. The *apparent* H_2/Zr sticking coefficient was reported[16] to be $s \approx 10^{-4}$. This low value in fact only characterizes the desorption probability [the true sticking coefficient measured for D_2 adsorption on Zr(0001) by employing the nuclear reaction analysis[8] was found to be high, $s = 0.38 \pm 0.16$ at $T = 300$ K (the true sticking coefficient for H_2 appears to be very similar to that for D_2)]. Shleifman *et al.*[14] have studied hydrogen desorption from Zr hydride in a chamber of small volume, which helped to improve the detection limit of the experiment. The temperature of the maximum in the desorption rate was about 800 K. With an increase of hydrogen concentration in the bulk, the desorption peak shifted to lower temperatures.

The volumes of the Zr foils employed in the above men-

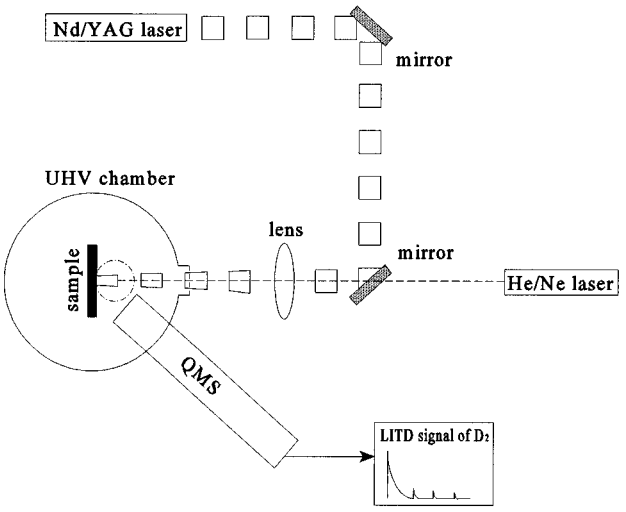

FIG. 1. Schematic of the LITD experimental setup.

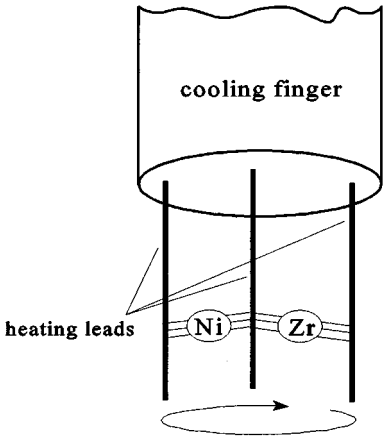

FIG. 2. Schematic of the sample holder of the Zr(0001) and Ni(110) samples.

tioned studies[5,14,16] were 10–50 times less than those of the monocrystal samples and they were heavily loaded with deuterium. The heating rates used[5,14,16] were ''conventional,'' ranging from 1 up to 100 K/s. With such heating rates, no hydrogen/deuterium desorption can be observed from the Zr monocrystals because the crystal capacity is high (the bulk had been depleted of dissolved H/D) and all the surface and subsurface hydrogen/deuterium rapidly diffuses into the bulk. In our LITD study, the heating rate was about 10^{11} K/s. With this heating rate, we were able to observe deuterium desorption from Zr(0001). The measured deuterium desorption probability, approximately 0.01, is in good agreement with the results of our calculations based on independent data available for the D/Zr(0001) system.

II. EXPERIMENT

The experiments were performed in a stainless-steel UHV chamber described elsewhere.[17] Briefly, the chamber was equipped with LEED, a mass spectrometer for temperature programmed desorption (TPD), Kelvin probe for work function change measurement, and Fourier transform infrared absorption reflection spectroscopy (FTIRAS). The typical background pressure was 2×10^{-10} Torr.

The schematic of the experimental setup for LITD is shown in Fig. 1. The surfaces were heated with laser pulses from a Quanta-Ray DCR Nd^{3+}/YAG (wavelength=1.06 μm). The beam profile had a donut-like shape and a Gaussian temporal distribution with FWHM of 10 ns. Pulses were guided with two dielectric mirrors and focused onto the surface with a lens (focal length=100 cm). The laser spot size (typically with 1.5 and 2.6 mm inner and outer diameter) was maintained the same in the experiments with Zr(0001) and Ni(110) (the latter sample has been used for calibration of the deuterium desorption yield as described below). The He/Ne laser beam was aligned externally with the Nd^{3+}/YAG laser pulses, enabling us to view the position of the infrared laser spot on the sample surface. In order to avoid desorption from chamber walls caused by reflected radiation, laser pulses entered and left the chamber via the same window.

In both cases (for Zr and Ni), the laser power was experimentally set below that which causes ablation of the surface. First, we found the minimum power for ablation on the reverse side of the crystal. The power was then gradually decreased until no damage could be observed even after several laser pulses on the same spot. The laser power determined in this way was then used for experiments on the front side of the crystals.

The elliptically-shaped samples were cut from a boule and aligned to within $\pm0.5°$ of the respective crystal planes using the standard Laue x-ray technique. The crystals were polished employing diamond and alumina pastes to 0.06 μm grades. The dimensions of the Ni(110) and Zr(0001) samples were $(10\times8\times1)$ mm and $(12\times6\times1.4)$ mm, respectively. Four platinum wires, each of 0.25 mm diameter, were spot-welded to the back of the crystals and suspended between two posts of the sample manipulator. A K-type thermocouple was spot welded to the back side of the samples, and a temperature controller was used to hold the crystal at any given temperature to within ±0.5 K by resistive heating. This arrangement provided rapid cooling down to 175 K, thus minimizing contamination during the cooldown. Both samples were mounted on the same cooling finger (Fig. 2), making possible identical geometrical conditions in the LITD experiments.

The Ni sample was cleaned by Ar^+ ion sputtering (3 kV, 5 μA) at room temperature for 15 min followed by annealing at 1273 K for 5 min. Residual carbon impurities were removed by exposure to several L of oxygen at room temperature followed by heating to 1273 K in 10^{-7} Torr D_2 for two to three minutes. The cleanliness of the surface was checked using the work function change after its saturation with deuterium at 175 K which has been shown to be extremely sensitive to surface impurities.[18]

Reproducible *absolute* hydrogen (deuterium) coverage on Ni(110) was prepared according to the method described

in Ref. 18. Slow cooling of the sample in H_2/D_2 (1×10^{-7} Torr) from $\simeq$400 K to 175 K results in a saturation coverage of 1.7 monolayers (ML) or 1.94×10^{15} H or D/cm^2 (if the crystal is exposed to H_2/D_2 at 175 K, the H/D coverage is only 1.49 ± 0.05 ML).

The cleaning procedure for Zr(0001) has been described elsewhere.[8] Briefly, the crystal was cleaned by 15-min sputtering cycles at 1023 K and at room temperature. The sample then was heated to 923 K and held for 2 min before each experiment to allow all residual impurities (O, C, etc.) and surface hydrogen to dissolve into the bulk and leave the surface free of any contamination.

III. EXPERIMENTAL RESULTS

As we have already pointed out in the Introduction, deuterium diffusion into the bulk of Zr is much faster compared to desorption. This makes it impossible to detect (by conventional TPD) any desorbing deuterium from the sample of typical thickness between 1–2 mm. To increase the desorption yield, we have heated the sample by laser pulses with a heating rate of 0.5 to 1.0×10^{11} K/s.

First, we have studied LITD from Zr(0001) free of deuterium in the bulk. The adsorbed overlayer was formed by dosing 4 L of D_2 at 175 K. These conditions were chosen because at 175 K deuterium only adsorbs on the surface and does not diffuse into the bulk.[10] Thus, we were able to observe the competition between desorption and diffusion in the situation when all the deuterium is on the surface at the start of the experiment (no contributions of bulk or of subsurface deuterium). To measure the deuterium desorption yield from Zr(0001) quantitatively, the data for Zr have been calibrated by comparing with the deuterium desorption yield from Ni(110) (in the latter case, the absolute deuterium coverage has been determined earlier by nuclear reaction analysis[18]). To eliminate the experimental uncertainty in the determination of the area of the laser spot on the surface, both samples were mounted on the same cooling finger of the manipulator (Fig. 2). The typical LITD signals of D_2 molecules from Zr(0001) and Ni(110) samples are shown in Fig. 3. The deuterium desorption yield measured for the Zr sample is in this case $\approx$0.01 ML.

Repeating the laser pulses, we have observed [both for Zr(0001) and Ni(110)] a series of LITD peaks with the intensity gradually decreasing to zero. All the signals following the first one appear to be caused by surface diffusion of deuterium into empty spots because bulk diffusion is not able to recover the surface coverage. For example, the diffusion coefficient of deuterium in the bulk of Zr at 175 K is 3.8×10^{-16} cm^2/s,[11] and the average diffusion length corresponding to 2 s (this is the interval between two pulses) is only 3 Å. This is less than the distance between two layers of Zr. On the other hand, the surface diffusion coefficients of deuterium on Ni(111) and Ni(100) are of the order of $10^{-8}-10^{-9}$ cm^2/s at 175 K.[19,20] Taking into account that the time between the first and second peak and the ratio of the integral intensities of these peaks are about the same for Zr and Ni, we conclude that the diffusion coefficient of deuterium on the Zr(0001) surface is of the same order of magnitude as that on the Ni surface. Thus, the ratio of surface and bulk diffusion coefficient at 175 K for Zr is very high, $\sim10^6-10^7$. This means that the empty spots formed after first and subsequent laser pulses are filled primarily via deuterium diffusion along the surface. Desorption from the chamber window or walls can be excluded by a blank experiment in which no LITD signal was detected from the clean surfaces of Zr and Ni. The deuterium concentration on the inner surface of the chamber was kept the same as in LITD experiment with deuterium covered sample surfaces. The clean surfaces were prepared by desorption and annealing the samples above the temperature of desorption.

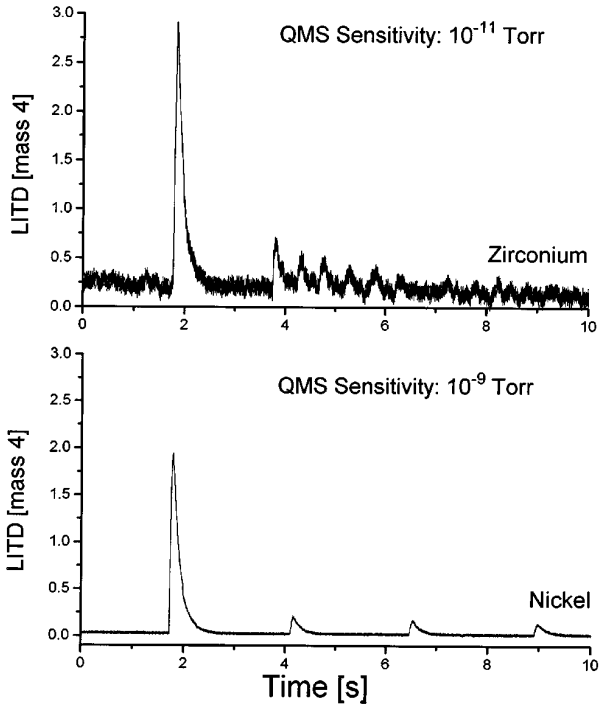

FIG. 3. LITD of D_2 from the bulk-clean Zr(0001) and Ni(110) samples for the sample temperature of 175 K.

In another experiment, the bulk of the Zr sample was loaded with deuterium by repeated adsorption/annealing cycles at 175 K (all the adsorbed deuterium is known[12] to diffuse in the bulk when the sample is slowly heated from this temperature up to 923 K). The final concentration of deuterium in the bulk ([D]/[Zr]), q_b, was 4×10^{-6}. Before every experiment, the sample was annealed at 923 K for 2 min and then cooled to 175 K or to room temperature. This procedure minimizes the surface concentration of deuterium. Nevertheless, some of deuterium always segregates to the surface and subsurface area during cooling, due to the higher binding energy in these regions compared to the bulk.[11] A LITD of deuterium from the Zr sample loaded by deuterium up to $q_b=4\times10^{-6}$ is shown in Fig. 4.

For experiments in which the D-loaded Zr sample was cooled to 175 K, deuterium predominantly desorbs in the first peak, as in the case when the sample is free of deuterium in the bulk. Comparing the normalized peak signals of the

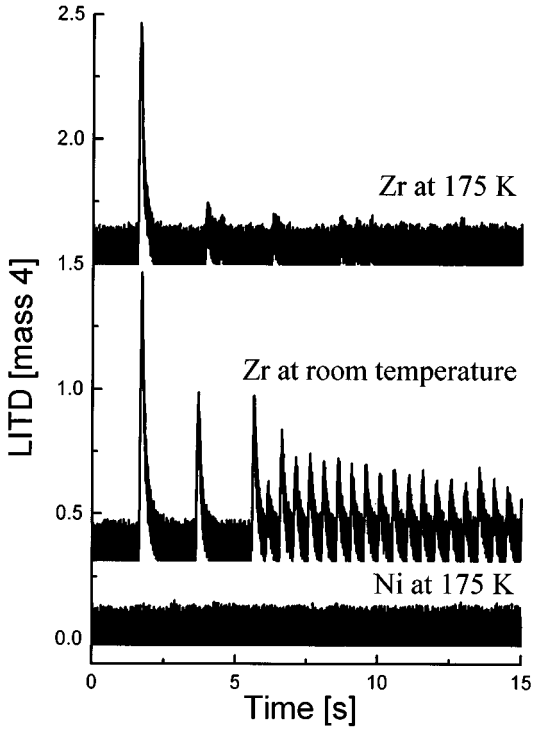

FIG. 4. LITD of D_2 from Zr(0001) loaded with D_2 ($q_b=4\times10^{-6}$) without exposure (i.e., for the sample annealed at 923 K before LITD) (i) at 175 K, (ii) at room temperature, and (iii) the blank experiment on Ni(110) at 175 K.

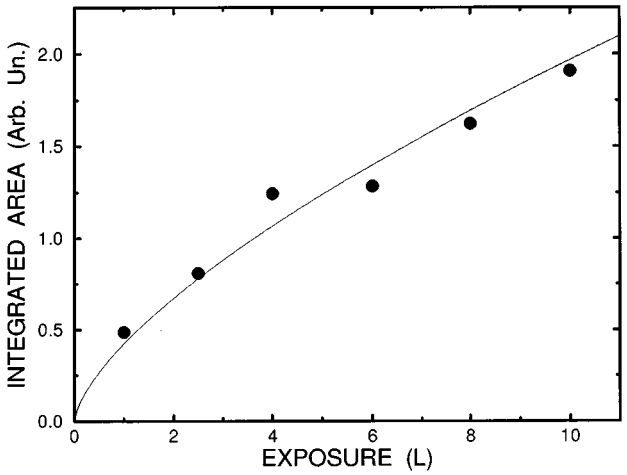

FIG. 5. Integrated area of the first LITD peak vs the D_2 exposure on Zr(0001) at room temperature and $q_b=4\times10^{-6}$. The filled circles show the experimental data. The solid line corresponds to interpolation $\mathscr{Y}\sim E^{2/3}$ (see the discussion in Sec. IV).

first three peaks for the two experimental conditions (with and without deuterium in the bulk), we conclude that the decrease of the signal is the same (within the range of the experimental error). Thus, the surface diffusion seems to be a dominant channel of filling the empty spots even if Zr is loaded with deuterium. In other words, the diffusion coefficient in the bulk at 175 K is so low that deuterium atoms are effectively ''frozen'' in the Zr lattice.

At room temperature (RT), the deuterium desorption yield for the first peak of the D-loaded Zr (without any deuterium exposure on the surface before LITD), 4×10^{-3} ML, is the same as that for 175 K (in the range of the experimental error). This indicates that a similar deuterium distribution on and near the surface seems to be established in both cases before the temperature drops (during cooling) to RT. On the other hand, the intensity of the second and subsequent LITD peaks is much higher than that for 175 K. This observation appears to be connected with additional filling of a bare surface due to bulk diffusion (the coefficient of deuterium diffusion in the bulk at RT is fairly high, 3.6×10^{-11} cm^2/s).

At RT, the ratio of the integrated areas of the second and third peak with respect to the first one are close, 0.55 and 0.54, respectively. The decrease in the intensity of subsequent peaks, however, becomes much stronger if the interval between peaks is decreased from 2 to, e.g., 0.5 s. In the latter case, the LITD signals gradually disappear because the bulk and surface diffusion are not able to recover the deuterium population on the spot irradiated.

The dependence of the desorption yield in the first peak on exposure to D_2 at RT for the sample loaded with deuterium ($q_b=4\times10^{-6}$) is shown in Fig. 5. The LITD signal increases with increasing exposure above 4 L regardless of the fact that the surface is close to saturation at 4 L.[8] At higher exposures, deuterium seems to diffuse into the subsurface region (the potential wells in this region are expected to be deeper than those in the bulk[10]). During LITD, subsurface deuterium atoms jump more or less at random in both directions (towards and away from the surface). Some of them are trapped by the surface and then diffuse again into the bulk. The total flux is of course directed into the bulk. But nevertheless these atoms slightly increase the population of the surface sites compared to the situation when the subsurface deuterium is lacking (simply because there is more deuterium on and near the surface in the former case). Accordingly, the desorption yield increases as well. Thus, although LITD is surface sensitive, subsurface deuterium also plays an important role in desorption.

Absolute values of second and subsequent LITD signals also increase at RT with increasing exposure. On the other hand, second-to-first peak area (SFPA) and third-to-first peak area (TFPA) ratios reach the same constant value at high exposures (Fig. 6). The SFPA ratio remains constant for exposures about 4 L. The TFPA ratio approaches a constant value at a higher exposure (about 10 L) because the ratio depends on the concentration and the distribution of subsurface deuterium. The higher the exposure, the more deuterium atoms diffuse into the bulk after the surface is saturated and the concentration difference between the surface and subsurface layers decreases. After desorption of the first peak from the saturated surface, the amount of deuterium which has diffused from the bulk to the bare surface is proportional to the subsurface concentration; this results in higher LITD yield in the second and following LITD peaks. Eventually (at high exposures), the concentration of subsurface deuterium seems to be so high that the SFPA and TFPA ratios become constant.

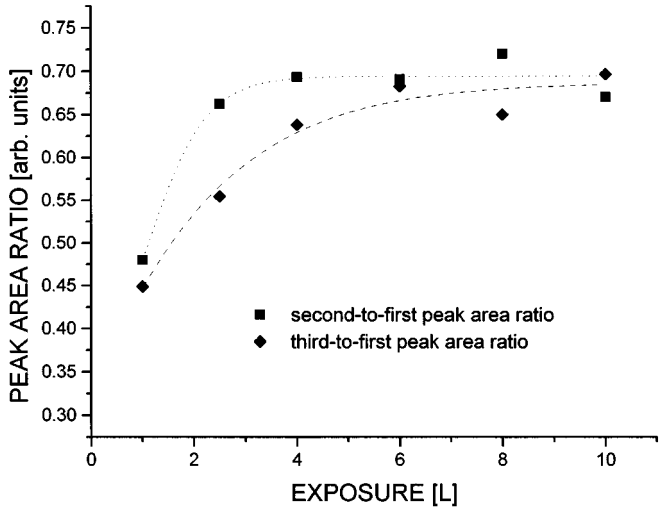

FIG. 6. Ratios of the integrated areas of the second and the third peak to that of the first peak as a function of exposure for LITD from the sample with $q_b=4\times10^{-6}$ at room temperature.

IV. RESULTS OF CALCULATIONS

The factor complicating the kinetics of hydrogen/deuterium desorption from Zr is connected with the possibility of the formation of hydride grains at low temperatures and their dissolution with increasing temperature. If the H/D concentration in Zr is low (lower than 1 at.%), all the hydrogen (or deuterium) should (at equilibrium) be in solution at temperatures above $\approx$500 K (see the H–Zr phase diagram[6]). Our calculations are oriented to the case when the H/D concentration is much lower than 1 at.%, and we will not analyze in detail the hydride dissolution kinetics. The latter is justified because (i) hydrogen/deuterium desorption occurs at relatively high temperatures, and (ii) during the transition from high to low surface coverages the surface and bulk are not in equilibrium and accordingly the desorption yield corresponding to this transition is fairly insensitive to the H/D concentration in the bulk [note, however, that in the course of conventional TPD measurements, the surface and bulk are close to equilibrium at very high temperatures when the surface coverage is low, $\theta_s<0.01$, and the desorption rate in the latter case is strongly dependent on θ_b (θ_b is the coverage corresponding to deep bulk layers)].

The experimental studies of deuterium segregation on the Zr(0001) surface indicate[10] that the potential barrier for jumps from the subsurface layer to the adsorbed overlayer is about the same as the potential barriers for diffusion in the bulk. In this case, the deuterium atoms which were able in the course of LITD to escape from the surface potential wells may easily be trapped again into these wells. Thus, the adsorbed overlayer and a few adjacent bulk layers should be in quasi-equilibrium already at the early stages of the transient kinetics. The latter makes it possible to simplify an analysis of the TPD kinetics. In particular, we can use Eq. (A14) derived in the Appendix. To apply this equation to deuterium desorption from Zr(0001), we need the rate constants for this process and also for deuterium diffusion in the bulk.

The Arrhenius parameters for associative desorption of deuterium from the Zr(0001) surface can be evaluated as follows. Considering that the sticking coefficient for D_2 on Zr(0001) is high, $s=0.38$, we conclude that the activated complex for D_2 adsorption and desorption has translational and rotational degrees of freedom. In this case, the preexponential factor for D_2 desorption is expected (from the transition state theory[2]) to be $\nu_{des}\approx10^{14}$ s^{-1}. The activation energy for desorption at low coverages, obtained from the enthalpy levels involved in the adsorption–desorption cycle, is given by

$$E_{des}=2(\Delta H_h-\Delta H_s+\Delta E)\approx46.8 \text{ kcal/mol}, \tag{1}$$

where $\Delta H_h=22.9$ kcal/mol is the heat of formation of the hydride phase (Ref. 6, p. 107), $\Delta H_s=9.0$ kcal/mol the difference between the heat of solution of deuterium in Zr and the hydride phase (Ref. 6, p. 94), and $\Delta E=9.5$ kcal/mol the segregation heat[10] at $\theta_s\ll1$.

Assuming the lattice for deuterium adsorption on Zr(0001) to be triangular and taking into account that the decrease of the segregation heat with increasing coverage up to saturation is about 3.5 kcal/mol (Ref. 10), we can estimate the nearest-neighbour adsorbate-adsorbate interaction as $\epsilon=3.5/z=0.58$ kcal/mol, where $z=6$ is the number of nearest-neighbour sites. Note that ''saturation'' ($\theta_s=1$) is defined here as the coverage corresponding to 1 ML (1 ML $\equiv1.11\times10^{15}$ atoms per cm^2).

The Arrhenius parameters for hydrogen diffusion in Zr are $\nu_{diff}\simeq3\times10^{11}$ s^{-1} and $E_{diff}=9.6$ kcal/mol (Ref. 11).

At low temperatures (below 200 K), diffusion into the bulk and desorption are very slow. In particular, if deuterium adsorption occurs at 175 K, all the deuterium atoms produced via dissociation of D_2 molecules stay at the surface. If the exposure is about 4 L (Fig. 3), the initial surface coverage is $\simeq$0.75 ML (Ref. 10). Conventional temperature-programmed kinetics ($\beta=100$ K/s) calculated for this initial condition with $\theta_b=0$ and 10^{-5} by employing Eqs. (A14) and (A16) with the set of parameters presented above are shown in Fig. 7 [Eq. (A16), derived for the case when desorption is absent, is more accurate in the corresponding limit than Eq. (A14)]. A few conclusions from these calculations are as follows. (i) The transition from high to low coverages takes place at $T\simeq450$ K. (ii) The surface coverage becomes low already at $T\simeq600$ K [we do not exhibit the results at $T>600$ because at very low surface coverages Eq. (A14) is not reliable]. (iii) The decrease in coverage with increasing temperature is primarily connected with diffusion into the bulk. Desorption in fact does not play any role. In particular, the desorption yield is lower than 3×10^{-7} ML at $T=600$ K (experimentally, desorption is not detected at these temperatures either for polycrystalline[5,16] or single-crystal[21] samples). (iv) The role of bulk deuterium is also minor at $T\leqslant600$ K (the kinetics for $\theta_b=0$ and 10^{-5} are in fact coincident). (v) The kinetics predicted by Eqs. (A14) and (A16) are in good agreement [taking into account that desorption in this case is negligible, we may conclude that the difference in the kinetics characterizes the accuracy of Eq. (A14)].

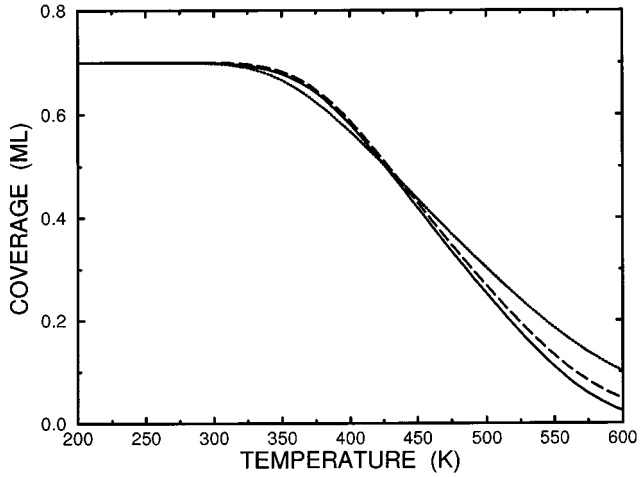

FIG. 7. Deuterium population of the Zr(0001) surface during heating at $\beta=100$ K/s: solid and dashed lines, Eq. (A14) with $\theta_b=0$ and $\theta_b=10^{-5}$, respectively [Eq. (A14) takes into account desorption and diffusion into the bulk]; dotted line, Eq. (A16) (no desorption). The initial temperature and coverage are 175 K and 0.75 ML, respectively.

If the metal surface is heated by pulsed-laser excitation, the absorbed energy is known[3,4] to be converted to thermal energy very rapidly ($\sim 10^{-13}$ s). Taking into account that the thermal diffusivity is much higher than the deuterium diffusion coefficient, one can then conclude that the temperature gradients in the region important for deuterium diffusion are negligible and employ the Ready equation[3] for calculating the time dependence of the temperature jump,

$$T(t)=T(0)+A(\pi ck)^{-1/2}I_m\int_0^t F(\tau)(t-\tau)^{-1/2}d\tau, \qquad (2)$$

where A is the absorptivity, c the heat capacity, k the thermal conductivity, I_m the maximum laser intensity, and $F(t)$ the temporal profile of the laser pulse. A typical time dependence of surface temperature for Zr is exhibited in Fig. 8 (in fact, the data presented correspond to the measurements shown in Fig. 3a). A rapid increase of temperature up to

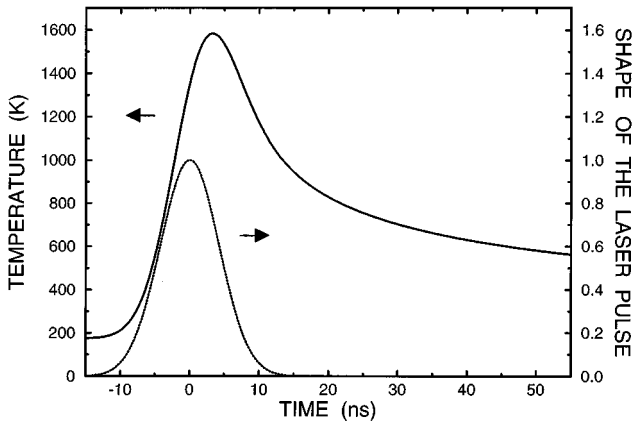

FIG. 8. Temporal profile of the laser pulse (Gaussian distribution with the FWHM of 10 ns) and Zr surface temperature [Eq. (2)] as a function of time. The parameters employed in the calculations are $I_m=14$ MW cm^{-2}, $A=0.68$ (Ref. 23), $c=1.75$ J cm^{-3} K^{-1}, and $k=0.227$ W cm^{-3} K^{-1}.

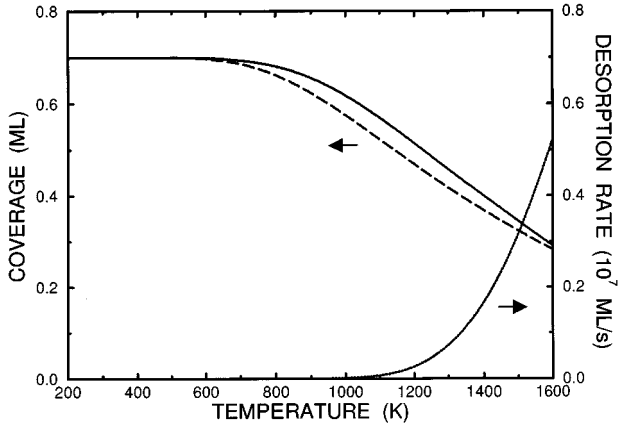

FIG. 9. Surface coverage [solid line, Eq. (A14); dashed line, Eq. (A16)] and desorption rate [Eq. (A14)] as a function of temperature for the D/Zr(0001) system with $\theta_b=10^{-5}$. The initial temperature and coverage are 175 K and 0.75 ML, respectively. The heating rate is 10^{11} K/s.

$\simeq 1600$ K is seen to be followed by a rapid fall down to 900 K. A further decrease in temperature is not so fast.

The time dependence of the surface coverage during the pulsed-laser heating of the surface is expected to be nonmonotonous. With increasing temperature, the surface coverage should rapidly decrease due to diffusion into the bulk and desorption. Just after reaching the maximum temperature, the coverage will increase a little due to diffusion back to the surface. Thereafter, the surface coverage will change in the direction of equilibrium with the bulk. Our analysis of the desorption/diffusion kinetics has shown that deuterium desorption occurs primarily during the initial stage when the temperature *increases* to its maximum value, because after reaching the maximum temperature the surface coverage is low. In addition, we have found that the bulk (with $\theta_b \leqslant 10^{-5}$) does not play any role in desorption. The latter conclusion, following from calculations, can also be illustrated simply by estimating a typical diffusion length, $l\simeq(D\tau)^{1/2}$, near the maximum temperature. With $T=1600$ K and $\tau\simeq 20$ ns, we get $l/a\simeq 20$ (a is the lattice spacing). Even if all the deuterium atoms which are able to reach the surface desorb, their contribution to the desorption yield, $\approx\theta_b l/a$, will be as low as $\approx 10^{-4}$.

As we have pointed out, deuterium desorption occurs primarily at the first stage of the temperature-programmed kinetics. In this case, the temperature increase (Fig. 8) is almost linear with $\beta\simeq 10^{11}$ K/s. The desorption/diffusion kinetics calculated with this heating rate by employing Eq. (A14) are shown in Fig. 9. The desorption yield given by these calculations is 0.008 ML. This value obtained *without any adjustable parameters* is in good agreement with the measured yield, $\simeq 0.01$ ML.

Above, we have discussed the diffusion/desorption kinetics in the case when the initial temperature is low, $T(0)=175$ K. Interpretation of the results of measurements obtained for $T(0)=300$ K is more complex because in this case deuterium starts to move from the surface into the bulk already during *adsorption*. Detailed analysis[10] of the deute-

rium adsorption kinetics indicates that the standard model, which assumes that all the bulk potential wells are equivalent (this model is used in the present work), slightly underestimates the deuterium uptake at high exposures. The latter seems to be connected with the extra uptake by a few subsurface layers (the potential wells corresponding to these layers appear to be deeper than those located in the bulk). Unfortunately, detailed data about the subsurface potential wells are lacking. For this reason, we have not tried to describe quantitatively the effect of such relatively deep wells on the adsorption or desorption kinetics. This shortcoming in simulations is not important for the *estimates* of the deuterium desorption yield. On the other hand, the subsurface potential wells might be crucial for understanding the dependence of the desorption yield upon exposure at 300 K (Fig. 5). The fact that the yield is approximately proportional to $E^{2/3}$ (E is exposure) cannot be simply explained in the framework of the standard model. If however we take into account a few relatively deep subsurface layers, the interpretation of this observation is quite straightforward. In particular, one can assume that deuterium, adsorbed at 300 K primarily on the surface, will be redistributed with increasing temperature among the surface and subsurface layers even at relatively low temperatures (before the onset of desorption). In this case, the coverage of all the layers will be relatively low, and equations (A1) and (A2) describing jumps between the layers (see the Appendix) will be linear. The latter means that all the coverages will simply be proportional to the uptake, $\theta_i \sim U$ (in particular, $\theta_s \sim U$). Considering that the rate of deuterium desorption is proportional to θ_s^2 one might conclude that the desorption yield, $\mathscr{Y}$, is proportional to U^2, i.e. $\mathscr{Y} \sim U^2$. On the other hand, the dependence of the uptake on exposure is[10] $U \sim E^{\alpha}$, where $\alpha \simeq 1/3$. Thus, we get $\mathscr{Y} \sim E^{2\alpha}$. This equation (with $\alpha \simeq 1/3$) explains why the desorption yield is approximately proportional to $E^{2/3}$.

Finally, it is reasonable to mention that at high temperatures one may in principle observe atomic desorption of deuterium. The preexponential factor for this process is expected to be of the same order of magnitude as that for molecular desorption. The activation energy for atomic desorption evaluated from the enthalpy levels is however very high,

$$E_{des}^{at} = (E_{des} + I)/2 \approx 75 \text{ kcal/mol}, \tag{3}$$

where $E_{des} = 46.8$ kcal/mol is the activation energy for molecular desorption, and $I = 103.3$ kcal/mol the D_2 dissociation energy. Thus, atomic desorption seems to be negligible (at least for $T < 1600$ K).

V. CONCLUSION

Our experimental and theoretical studies of the kinetics of temperature-programmed desorption of deuterium from Zr demonstrate that the desorption yield which is suppressed by adsorbate diffusion into the solid, can be considerably increased by increasing the heating rate from ''conventional'' values ($\beta \leqslant 100$ 100 K/s) to those ($10^{10} - 10^{11}$ K/s) corresponding to pulsed-laser thermal excitation. Thus, the LITD technique can successfully be employed in situations which are almost hopeless for conventional TPD measurements. Finally, we may also conclude that the surprisingly-good *quantitative* agreement between theory (without any adjustable parameters) and experiment indicates that modeling works under well-controlled conditions.

ACKNOWLEDGMENTS

The authors would like to thank G. Bickle, L. Green, B. Kasemo, and C.-S. Zhang for many stimulating discussions. M. K. acknowledges the award of the NATO Science Fellowship. V. P. Zh. thanks the Royal Swedish Academy of Sciences for supporting his stay at Chalmers University of Technology. Support from the Candu Owner's Group is also greatfully acknowledged.

APPENDIX: GENERAL EQUATIONS

The temperature-programmed kinetics of dissociative adsorption accompanied by adsorbate diffusion into the solid have been analyzed in Ref. 2 (Chap. 5.2). The model employed was based on the assumption that the jumps from the surface to the subsurface layer are irreversible. Below, the concurrent kinetics of desorption and diffusion are considered in more detail. In particular, the equations derived take into account reversibility of diffusion into the bulk.

In general, desorption accompanied by adsorbate diffusion into the solid is described by an infinite set of ordinary differential equations for the populations of the surface and bulk layers,

$$\frac{d\theta_s}{dt} = k_{10}\theta_1 - k_{01}\theta_s - k_{des}\theta_s^2, \tag{A1}$$

$$\frac{d\theta_i}{dt} = k_{i-1,i}\theta_{i-1} - (k_{i,i-1} + k_{i,i+1})\theta_i + k_{i+1,i}\theta_{i+1}, \tag{A2}$$

where θ_s is the coverage corresponding to the surface layer, θ_i ($i \geqslant 1$) the coverages of the bulk layers, k_{ij} the rate constants for the transitions from layer i to layer j, and $k_{des}\theta_s^2$ the desorption rate. In the course of thermal desorption, the temperature increases with increasing time, $T(t) = T(0) + \beta t$. Thus, all the rate constants in the equations above are implicitly (through temperature) dependent on time.

Assuming the population of the bulk layers to be low ($\theta_i \ll 1$), we neglect the coverage dependence of the rate constants for transitions between these layers. On the other hand, the adsorbed overlayer may be close to saturation, and we should take into account the dependence of the rate constants k_{10}, k_{01}, and k_{des} on the surface coverage. This dependence may be strong due to lateral adsorbate–adsorbate interactions. In general, one needs to distinguish lateral interactions in the ground and activated states[2] (the terms ''ground'' and ''activated'' correspond to the transition state theory). In our calculations, the interactions in the activated state are neglected (if necessary, one may easily take into

account the latter interactions). Employing the quasi-chemical approximation to take into consideration the lateral interactions in the ground state, we have[2]

$$k_{10}=(1-\theta_s)\,\nu_{dif}\,\exp(-E_{10}/T), \tag{A3}$$

$$k_{01}=\nu_{dif}\,\exp(-E_{01}/T)S^z, \tag{A4}$$

$$k_{des}\theta_s^2=\nu_{des}\,\exp(-E_{des}/T)\mathscr{P}_{AA}S^{2z-2}, \tag{A5}$$

and

$$S=\frac{\mathscr{P}_{AA}\,\exp(\epsilon/T)+0.5\mathscr{P}_{AO}}{\mathscr{P}_{AA}+0.5\mathscr{P}_{AO}}, \tag{A6}$$

where ν_{dif}, ν_{des}, E_{10}, E_{01}, and E_{des} are the Arrhenius parameters for diffusion and desorption (the activation energies E_{01} and E_{des} correspond to the low-coverage limit, $\theta_s \ll 1$; note also that $k_B=1$), ϵ the nearest-neighbour lateral interaction, z the number of nearest-neighbour sites, and $\mathscr{P}_{AA}$ and $\mathscr{P}_{AO}$ the well-known quasi-chemical probabilities to find a pair of sites occupied by two or one particle, respectively.

The type of approximations which can be used for solving Eqs. (A1) and (A2) depends on the behaviour of the potential energy for diffusion. Our attention will be focused on the situation when the surface potential wells are much deeper than the potential wells in the bulk and in the subsurface region. In this case, corresponding to many real systems, the formalism employed is quite different depending on the ratio between the activation energies for the bulk diffusion and for jumps from the subsurface layer to the adsorbed overlayer.

The set of equations is simplest if the former activation energy is much lower than the latter one. In this limit, equilibration of all the bulk layers is very fast. In particular, the subsurface layer is in fact in equilibrium with the bulk. Considering for simplicity that the subsurface potential wells are the same as in the bulk, we have $\theta_1=\theta_b$, where $\theta_b \ll 1$ is the coverage corresponding to the bulk layers. Then, replacing θ_1 in Eq. (1) by θ_b yields

$$d\theta_s/dt=k_{10}\theta_b-k_{01}\theta_s-k_{des}\theta_s^2. \tag{A7}$$

This equation has been used in Refs. 1 and 2.

The other important tractable limit (relevant for the D/Zr system) occurs if the activation energies for the bulk diffusion and for jumps from the subsurface layer to the adsorbed overlayer are comparable. In the latter case, the particles which were able to escape from the surface potential wells may easily be trapped again into these wells. Thus, it is clear that the adsorbed overlayer and several adjacent bulk layers should be in quasi-equilibrium already at the early stages of the transient kinetics, i.e.

$$\theta_s=\alpha(\theta_s)\,\theta(0,t), \tag{A8}$$

where $\theta(0,t)$ is the coverage of bulk layers near the surface, and $\alpha(\theta_s)$ the equilibrium constant corresponding to a given value of the surface coverage.

Replacing the infinite set of ordinary differential equations for coverages corresponding to bulk layers by the diffusion equation and employing Eq. (A8) as the boundary condition for the latter equation, one can simplify the analysis of the problem under consideration (see a detailed discussion[10] concerning the kinetics of adsorption accompanied by diffusion into the solid). In particular, Eq. (A1) can be rewritten as

$$\frac{d\theta_s}{dt}=-J-k_{des}\theta_s^2, \tag{A9}$$

where J is the diffusion flux near the surface. The latter flux can in principle be calculated self-consistently by solving Eq. (A1) together with an integral equation for J, obtained from the differential diffusion equation. An accurate solution of the integral equation is however difficult. For this reason, we will employ (in analogy with Ref. 10) the following approximation for the diffusion flux:

$$J\simeq D(t)[\theta(0,t)-\theta_b]/[a\,l(t)], \tag{A10}$$

where $D(t)=a^2k(t)$ is the diffusion coefficient (k the jump rate for the bulk layers, i.e., $k\equiv k_{i,i+1}$ for $i\gg 1$), $\theta(0,t)-\theta_b$ the difference of coverages of the bulk layers near and far from the surface, a the lattice spacing, and $l(t)$ the characteristic diffusion length at a given time. Physically, Eq. (A10) is quite clear (the right-hand part of this equation is simply a product of the diffusion coefficient and the scale of the concentration gradient).

Substituting expression (A10) into Eq. (A9) and taking into account condition (A8), we have

$$\frac{d\theta_s}{dt}=\frac{D(t)[\theta_b-\theta_s/\alpha(\theta_s)]}{a\,l(t)}-k_{des}\theta_s^2. \tag{A11}$$

The diffusion length $l(t)$ figuring in Eqs. (A10) and (A11) can be defined as

$$l(t)=[D(t)\,\tau(t)]^{1/2}, \tag{A12}$$

where $\tau(t)$ is the characteristic time for diffusion at a given time t. At the isothermal conditions, one can usually consider[10] that $\tau(t)=t$. For the temperature-programmed regimes, the situation is quite different because the diffusion coefficient rapidly increases with increasing time due to the temperature rise. For this reason, the propagation of diffusing particles occurs primarily during a narrow time interval located just below t. In this region, we have

$$\begin{aligned} D(t+\Delta t)&=\nu_{dif}a^2\,\exp[-E_{dif}/(T(t)+\beta\Delta t)] \\ &\approx D(t)\exp[E_{dif}\beta\Delta t/T^2(t)]. \end{aligned} \tag{A13}$$

The latter equation shows that the characteristic time for diffusion is given by $\tau(t)\approx T^2(t)/\beta E_{dif}$. Inserting this expression into Eq. (A12) and then substituting the result obtained by Eq. (A11) yields

$$\frac{d\theta_s}{dt}=\left[\frac{D(t)\beta E_{dif}}{a^2T^2(t)}\right]^{1/2}\left[\theta_b-\frac{\theta_s}{\alpha(\theta_s)}\right]-k_{des}\theta_s^2. \tag{A14}$$

To integrate Eq. (A14), one needs explicit expressions for the desorption rate and equilibrium rate constant. In the framework of the quasi-chemical approximation, the former is given by Eq. (A5) and the latter is represented as[2,22]

$$\alpha(\theta_s)=\exp(\Delta E/T)(1-\theta_s)S^{-z}, \tag{A15}$$

where ΔE is the segregation heat at $\theta_s \ll 1$, and S the factor defined by Eq. (A6).

Equation (A14) derived above is an approximation to the integral equation describing diffusion. It has been obtained for the case when the diffusion flux is directed from the surface. In addition, the diffusion flux has been assumed to be primarily governed by the change in the surface coverage. The latter is not the case if the surface coverage is very low. To understand the limits of applicability of Eq. (A14), we have compared the kinetics predicted by this equation in the situation when desorption is lacking with those given for this case by a more accurate solution to the integral equation for diffusion,[22]

$$\frac{\theta_s(t)}{\alpha[\theta_s(t)]}=\theta_b-\frac{a[\theta_s(t)-\theta_s(0)]}{[\pi D(t)T^2/\beta E_{dif}]^{1/2}}. \tag{A16}$$

Our experience indicates (see, e.g., Sec. IV) that Eq. (A14) can be employed down to $\theta_s \approx 0.01$.

Finally, it is of interest to note that the structure of Eq. (A14) is the same as that of Eq. (A7). In particular, Eq. (A14) can be rewritten as

$$\frac{d\theta_s}{dt}=k_{10}^{ef}\theta_b-k_{01}^{ef}\theta_s-k_{des}\theta_s^2, \tag{A17}$$

where $k_{10}^{ef}=[D(t)\beta E_{dif}/a^2T^2(t)]^{1/2}$ and $k_{01}^{ef}=[D(t) \times \beta E_{dif}/a^2T^2(t)]^{1/2}/\alpha(\theta_s)$ are the effective rate constants. Analogy between Eqs. (A7) and (A17) opens up the possibility to construct an unique classification of the temperature-programmed kinetics predicted by these equations.

[1] R.J. Borg and G.J. Dienes, *The Physical Chemistry of Solids* (Academic Press, Boston, 1992), Chap. 11.8.
[2] V.P. Zhdanov, *Elementary Physicochemical Processes on Solid Surfaces* (Plenum, New York, 1991), Chaps. 4.2 and 5.2.
[3] R.B. Hall, J. Phys. Chem. **91**, 1007 (1987).
[4] R.J. Levis, Annu. Rev. Phys. Chem. **45**, 483 (1994).
[5] J.S. Foord, P.J. Goddard, and R.M. Lambert, Surf. Sci. **94**, 339 (1980).
[6] D.O. Northwood and U. Kosasih, Int. Meteorol. Rev. **28**, 92 (1983).
[7] M. Yamamoto, S. Naito, M. Mabuchi, and T. Hashino, J. Phys. Chem. **96**, 3409 (1992).
[8] C.-S. Zhang, B.J. Flinn, K. Griffiths, and P.R. Norton, J. Vac. Sci. Technol. A **10**, 2560 (1992).
[9] C.-S. Zhang, B.J. Flinn, and P.R. Norton, J. Nucl. Mat. **199**, 231 (1993).
[10] B. Li, C.-S. Zhang, V.P. Zhdanov, and P.R. Norton, Surf. Sci. **322**, 373 (1995).
[11] C.-S. Zhang, B. Li, and P.R. Norton, J. Alloy Compound **231**, 354 (1995).
[12] C.-S. Zhang, B. Li, and P.R. Norton, Surf. Sci. **346**, 206 (1996).
[13] S. Naito, J. Chem. Phys. **79**, 3113 (1993).
[14] D.E. Shleifman, D. Shaltiel, and I.T. Steinberger, J. Alloy Compound **223**, 81 (1995).
[15] C.-S. Zhang, B.J. Flinn, and P.R. Norton, Surf. Sci. **264**, 1 (1992).
[16] J.-M. Lin and R.E. Gilbert, Appl. Surf. Sci. **18**, 315 (1984).
[17] B .W. Callen, K. Griffiths, U. Memmert, D.A. Harrison, S.J. Bushby, and P. R. Norton, Surf. Sci. **230**, 159 (1990).
[18] T.E. Jackman, K. Griffith, W.N. Unertl, J.A. Davies, K.H. Gurtler, D.A. Harrington, and P. R. Norton, Surf. Sci. **179**, 297 (1987).
[19] T.-S. Lin and R. Gomer, Surf. Sci. **255**, 41 (1991).
[20] S.M. George, A.M. DeSantolo, and R.B. Hall, Surf. Sci. **159**, L425 (1985).
[21] C.-S. Zhang (private communication).
[22] V.P. Zhdanov and P.R. Norton, J. Chem. Phys. **101**, 8200 (1994).
[23] Y.S. Toulokin and D.P. DeWitt, *Thermal Radiative Properties: Metallic Elements and Alloys* (Plenum, New York, 1970), Vol. 7, p. 883.